New diagnostics of Solar Eruptions with future Visible Light and UV HI Lyα Coronagraphs

A. Bemporad[1] and the Metis Team
[1]INAF – Osservatorio Astrofisico di Torino

Outline

1. Quick theoretical recap
2. Tests with real observations of CMEs
3. Tests with synthetic observations of CMEs
4. Summary

1) Quick theoretical recap

Plasma diagnostics from WL and UV coronagraphy

• **WL** emission of **K-corona** (F-corona removed) is due to **Thomson scattering** of photospheric radiation by coronal electrons resulting in **partially polarized emission**:

$$pB(\rho) = \frac{\pi}{2}\sigma_T \bar{B}_\odot \int_{-\infty}^{+\infty} n_e(z) \left[\frac{(1-u)A(r)+uB(r)}{1-u/3}\right] \frac{\rho^2}{r^2} dz$$

σ_T Thomson scattering | $B_\odot$ solar WL brightness | u WL limb darkening | $A(r)$, $B(r)$ geometric coefficients | $\rho(r)$ projected altitude

• The WL depends only on the LOS distirbution of ne → with standard (Van de Hulst) inversion WL images will be used to **measure n_e** .

• **UV** HI Ly-α emission in **stationary** corona (≠ CMEs) is almost entirely due to **radiative excitation** of H atoms by chromospheric radiation, followed by spontaneous emission (Gabriel 1971):

$$P_{gj}^{rad} = 0.83\, h\nu_{gj} B_{gj} \int_\Omega p(\phi) \int_{\mathbf{v}} f(\mathbf{v}) R(T_e) A_X\, n_e \int_0^\infty \Psi(\nu-\nu_0) I_{disk}(\nu', \mathbf{n}') d\nu d^3 v \frac{d\omega'}{4\pi}$$

$p(\varphi)$ redistribution function | $f(\mathbf{v})$ velocity distribution | $R(T_e)$ Ionization ratio | Ψ coronal atomic absorption profile | I_{disk} chromospheric excitation profile

• The intensity of the line also depends on plasma **electron density and temperature** (→ neutral H fraction), **proton kinetic temperature** (→ atomic absorption profile) and **proton velocity distribution** (→ Doppler dimming) integrated along the **line of sight** (LOS) → under specific assumptions combined WL-UV images can be used to **measure T_e and/or v_{out}**.

Lyman-α Doppler dimming

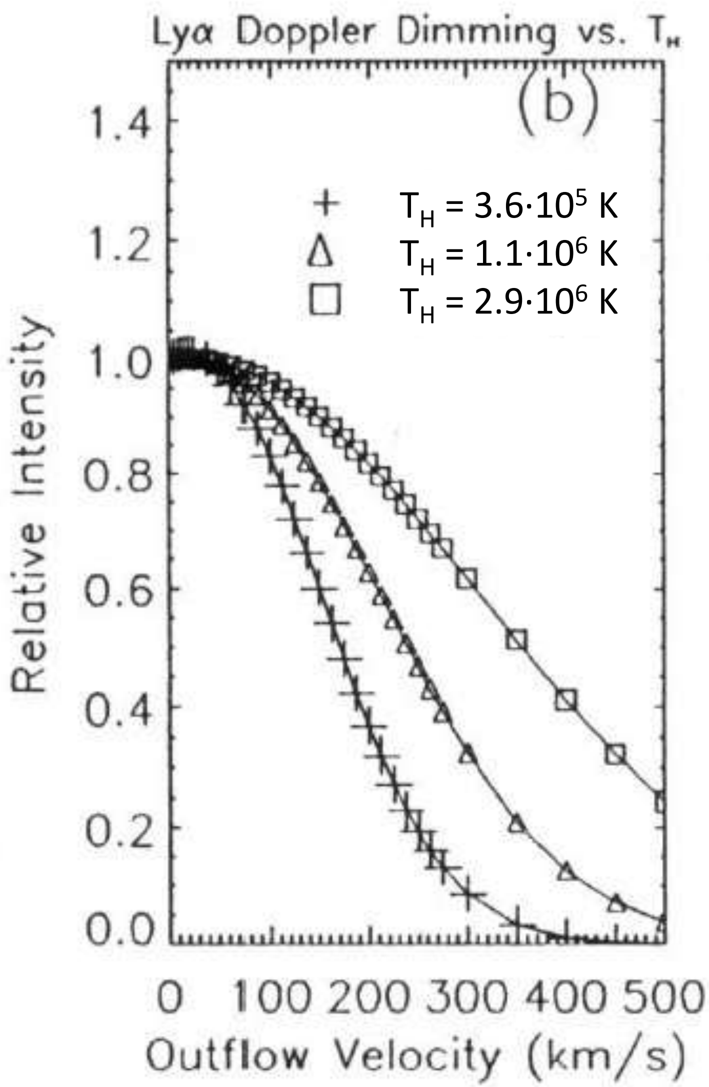

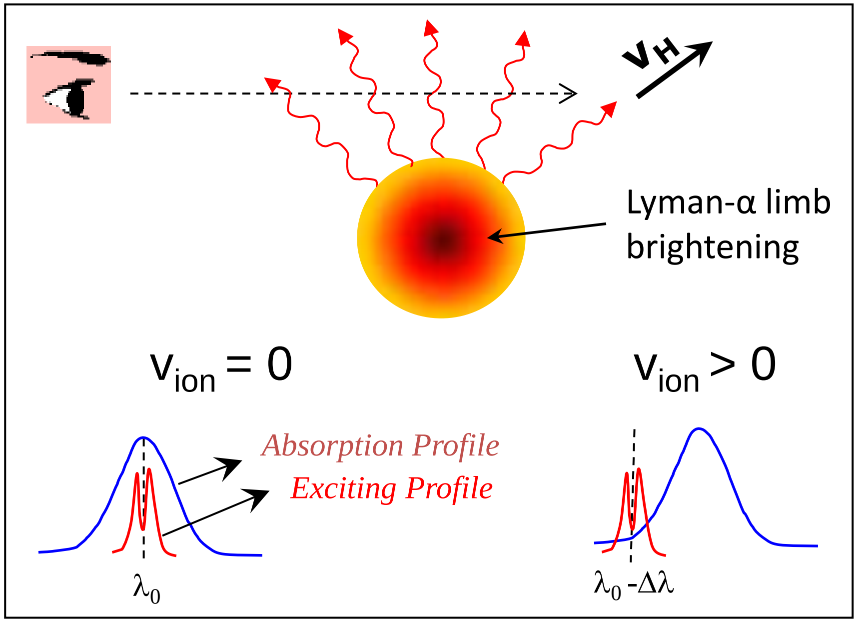

$$F(\delta\nu) = \int_0^\infty I_{disk}(\nu - \delta\nu)\,\Psi(\nu - \nu_0)\,d\nu$$

$$D = \frac{\int_\Omega F(\delta\nu)\,p(\phi)\,d\omega'}{\int_\Omega F(0)\,p(\phi)\,d\omega'}$$

Doppler dimming factor ($0 \le D \le 1$)

$D_{Ly\alpha}(v_{out} > 500$ km/s$) \sim 0$

Lyα Doppler dimming limit

Doppler dimming technique in CMEs

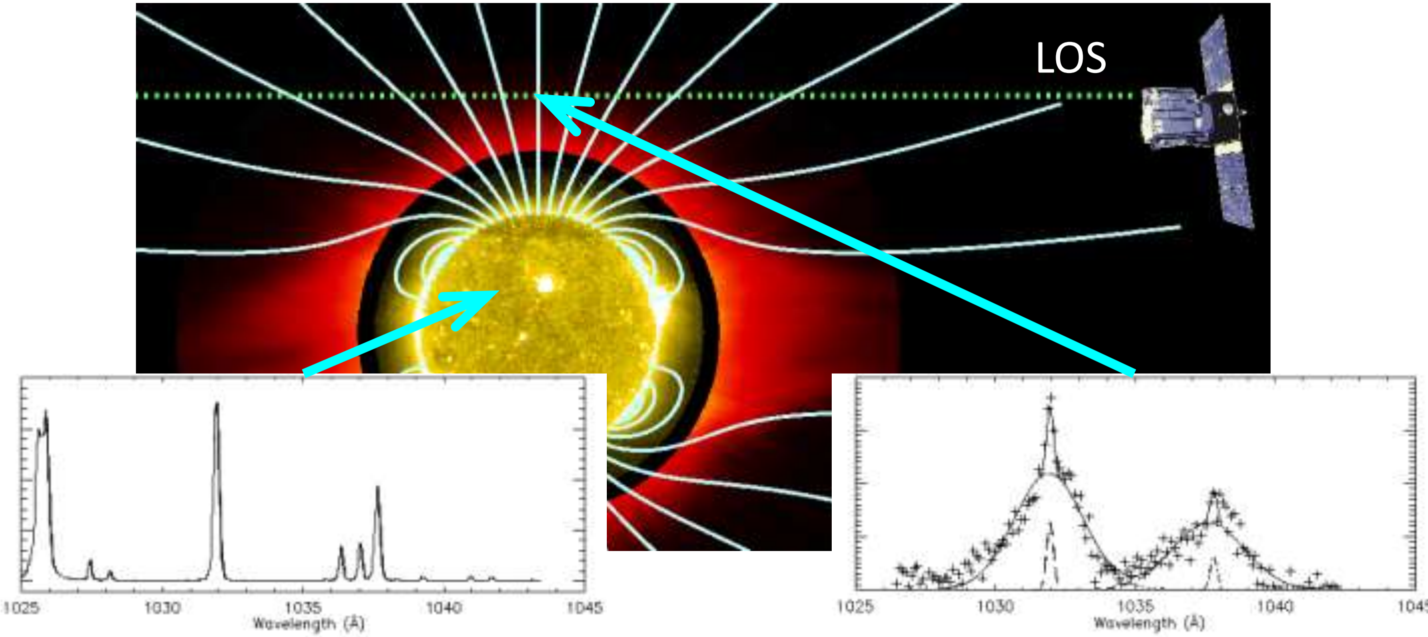

On-disk profiles: T = 1–3 MK

Off-limb profiles: **T > 200 MK!**

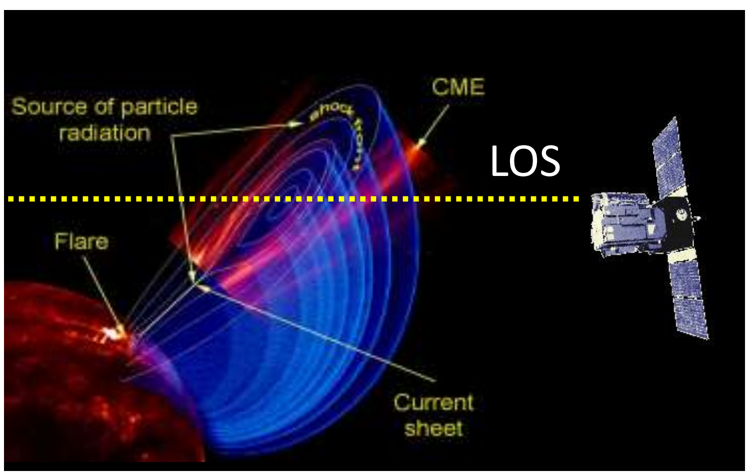

Doppler dimming technique in coronal stationary structures requires knowledge of LOS distribution of outflows, magnetic fields, T_e, T_{para} and T_{perp}, etc... These parameters can be constrained with models.

For CMEs this is very hard because their internal structure is not yet understood and each event has peculiar properties.

Usual assumptions: foreground and background coronal emission negligible with respect to the CME emission, LOS integration effects often negligible, $T_{para} = T_{perp}$, $v_{LOS}(z) = v_{POS}$

New diagnostics for CMEs: workflow

Previous works based on UVCS data took advantage of spectroscopic information to measure plasma density and temperatures (electron, kinetic, non-thermal broaqdenings). In the last decade we **investigated** how the **combination of co-spatial and co-temporal WL and UV Lyα intensities** (without spectroscopic info) can be analyzed to improve our knowledge of CMEs.

Studies of **CMEs** with combined WL and UV Lyα intensities

First tests with UVCS & MLSO MK3 observations of a slow CME (Bemporad et al. 2007)

→ Furthers tests with UVCS & LASCO observations of 3 CMEs (Susino & Bemporad 2016)

→ Analysis of LASCO data to constrain CME 2D speed and Doppler dimming (Ying et al. 2019 – in progress)

Studies of **shock waves** with combined WL and UV Lyα intensities

First tests analyzing UVCS & LASCO data with MHD Rankine-Hugoniot eq. (Bemporad & Mancuso 2010)

→ Furthers tests with UVCS & LASCO data (Bemporad, Susino & Lapenta 2014)

→ Comparisons with numerical simulations (Bacchini et al. 2015)

Studies of **erupting prominences** with combined WL and UV Lyα intensities

First tests with UVCS & LASCO data taking into account plasma optical thickness in UV (Heinzel et al. 2016)

→ Furthers tests with UVCS & LASCO data (Jejčič et al. 2017; Susino et al. 2018)

Optimization of plasma diagnostics with **numerical simulations**

First tests with synthetic VL data to improve density estimate (Bemporad & Pagano 2015; Pagano et al. 2015)

→ Further tests with synthetic VL and UV data to estimate temperature s (Bemporad, Pagano & Giordano 2018)

2) Tests with real observations of CMEs

Testing combination of WL and UV Lyα

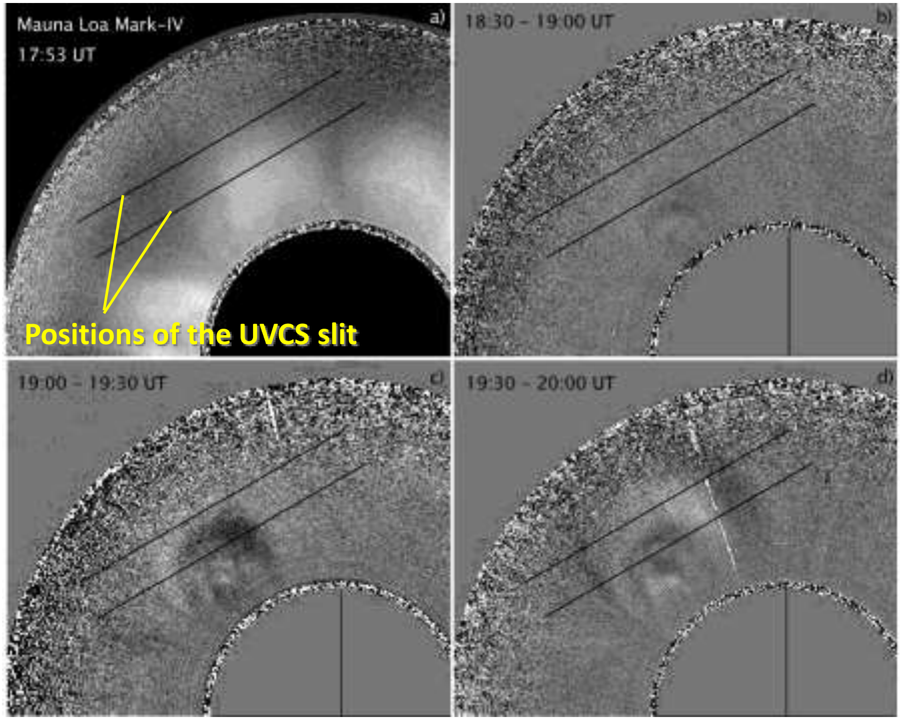

Mark-IV running difference images

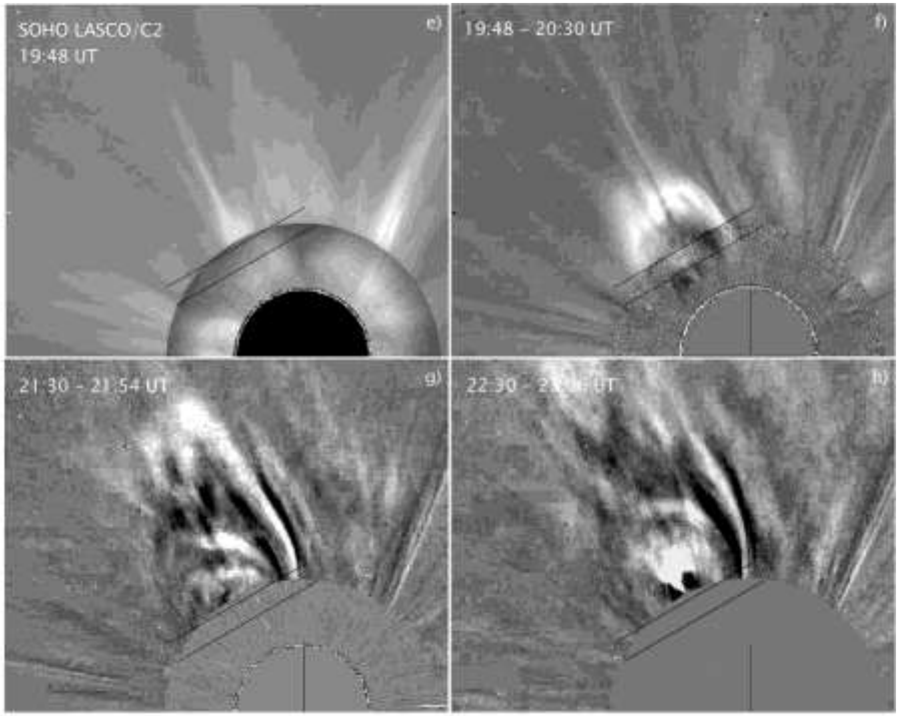

LASCO C2 running difference images

Position: UVCS slit center alternatively at **1.6** and **1.9** $\mathbf{R_\odot}$ at a latitude of 60°N
Time coverage: 2000/31/01, 17:06 → 2000/01/02, 02:00 (~**9 hours**)
Main spectral lines observed: H Lyα and Lyβ, O VI doublet, Si XII

UVCS slit **centered at the CME latitude → transit of the whole CME bubble observed**

(Bemporad et al. 2007)

WL and UV Lyα observations of CMEs

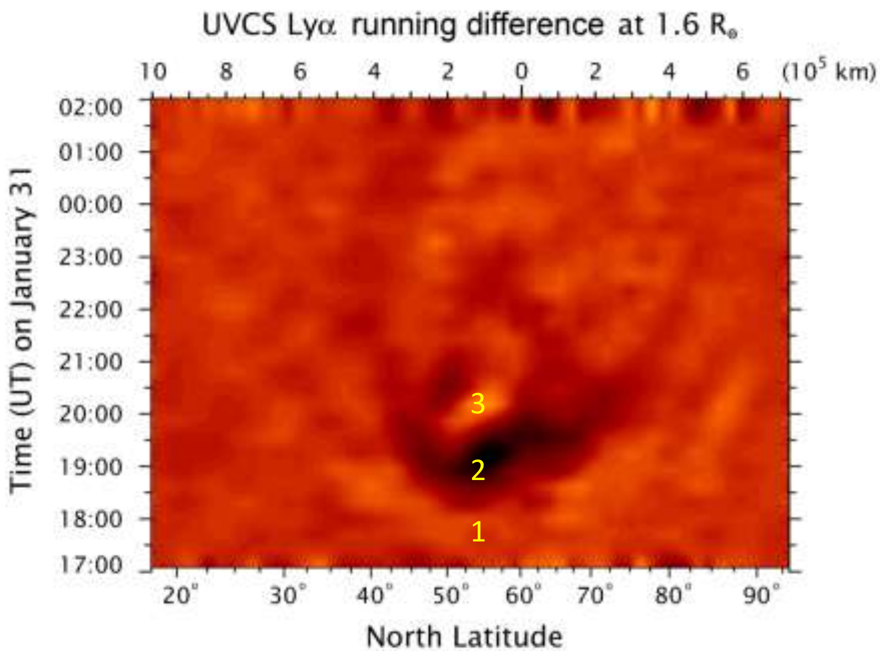

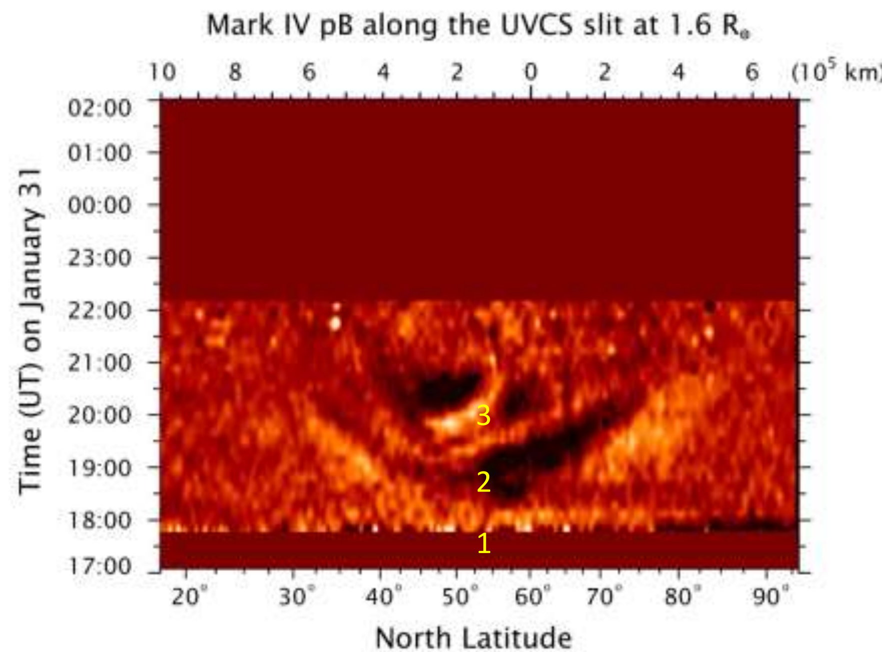

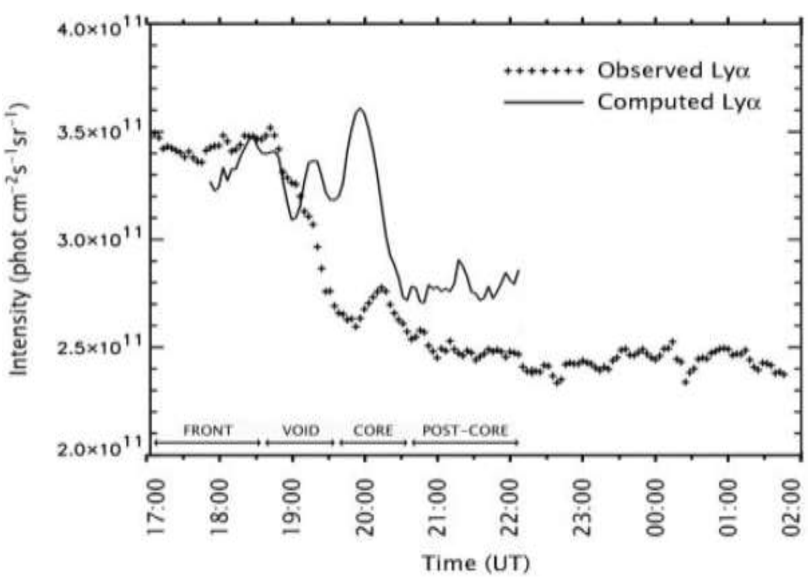

First example of possible Metis CME analysis:

1) CME densities derived from WL (MarkIV)
2) CME front: HI Ly-α intensities (UVCS) well reproduced from measured densities with v_{out} = 30 km/s (slow CME) and T_e = $10^{6.3}$ K
3) CME core: HI Ly-α intensity lower than expected → larger T_e = $10^{6.45}$ K (no erupting prominence)

Demonstrates feasibility of this analysis and shows potential of combining WL and UV data!

WL and UV Lyα observations of CMEs

- We selected three events observed simultaneously by LASCO-C2 and UVCS

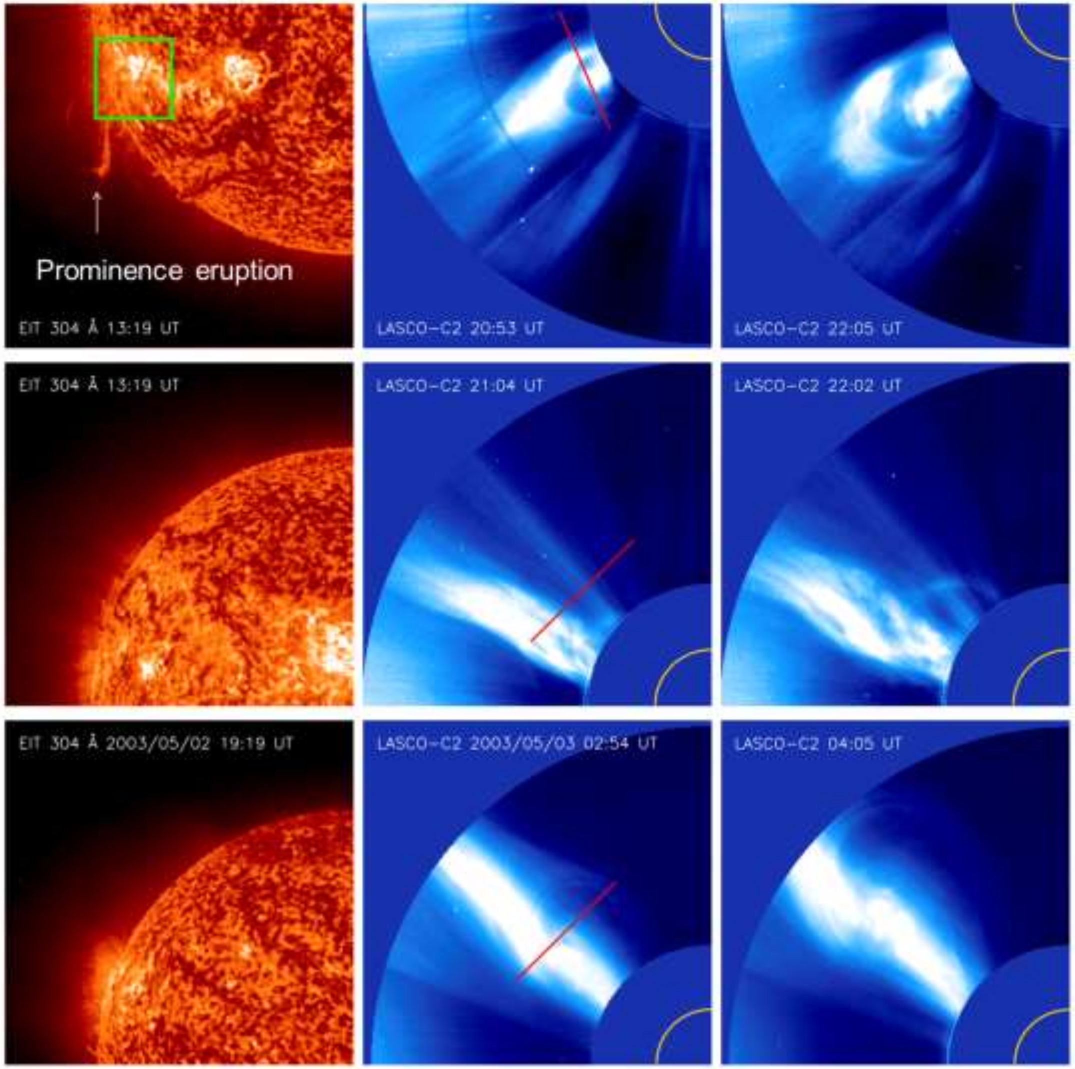

TEST CASE
2000 November 8: **narrow, slow CME** (v_{POS} ~ 160 km/s) with typical **three-part structure**, associated with a prominence eruption
UCSV slit @ 2.5 $R_\odot$

2000 December 25: **small-scale streamer blowout** triggered by an adjacent CME, with an estimated velocity of ~ 250 km/s
UCSV slit @ 3.0 $R_\odot$

2003 May 2-3: **faint CME with typical three-part structure** propagating inside a large and bright mid-latitude coronal streamer with velocity ~ 200 km/s
UCSV slit @ 3.5 $R_\odot$

(Susino & Bemporad et al. 2016)

WL and UV Lyα observations of CMEs

- CME front and core plasma is concentrated at an **average distance of ~ 1.6 R⊙** from the POS → **average POS angle of ~ 30°** consistent with source AR location
- Larger distances in the surrounding regions → LOS density distribution in the void and quiet corona is **likely broad**
- Electron densities are in the range ~ 10^6–10^7 cm^{-3}, **consistent with values measured** for CMEs
- **Latitudinal correlation** between the distribution of the electron density and that of Lyman-α intensity

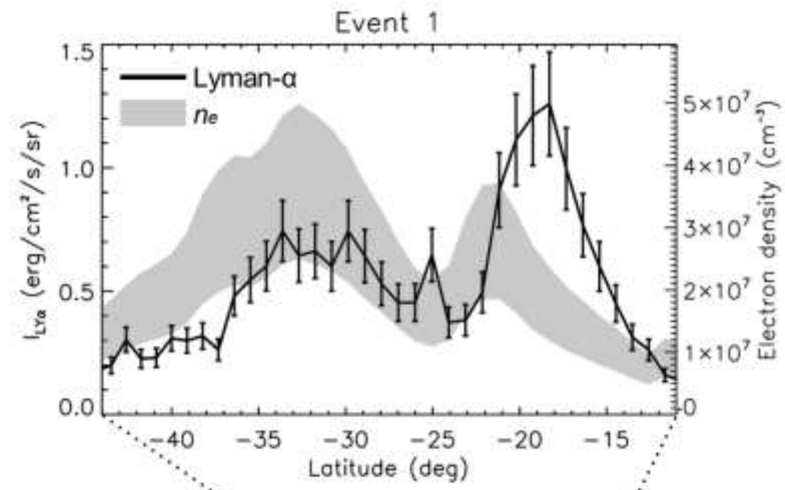

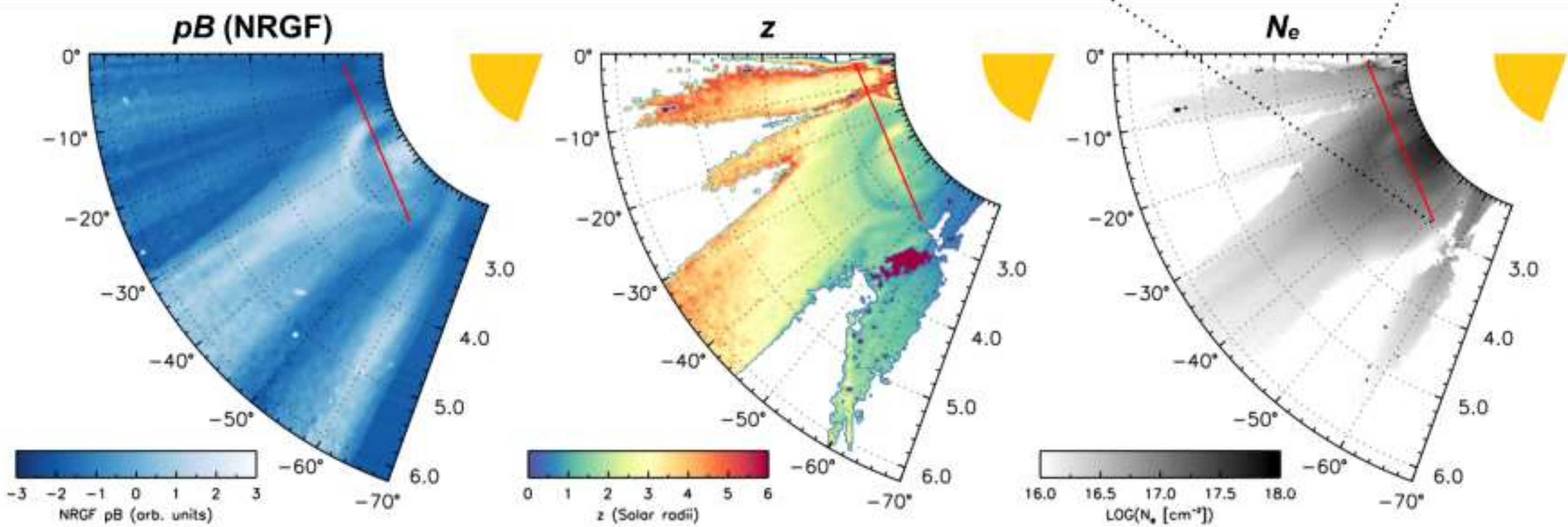

2D distribution of CME speed on the POS

LASCO-C2 *tB* (filtered)

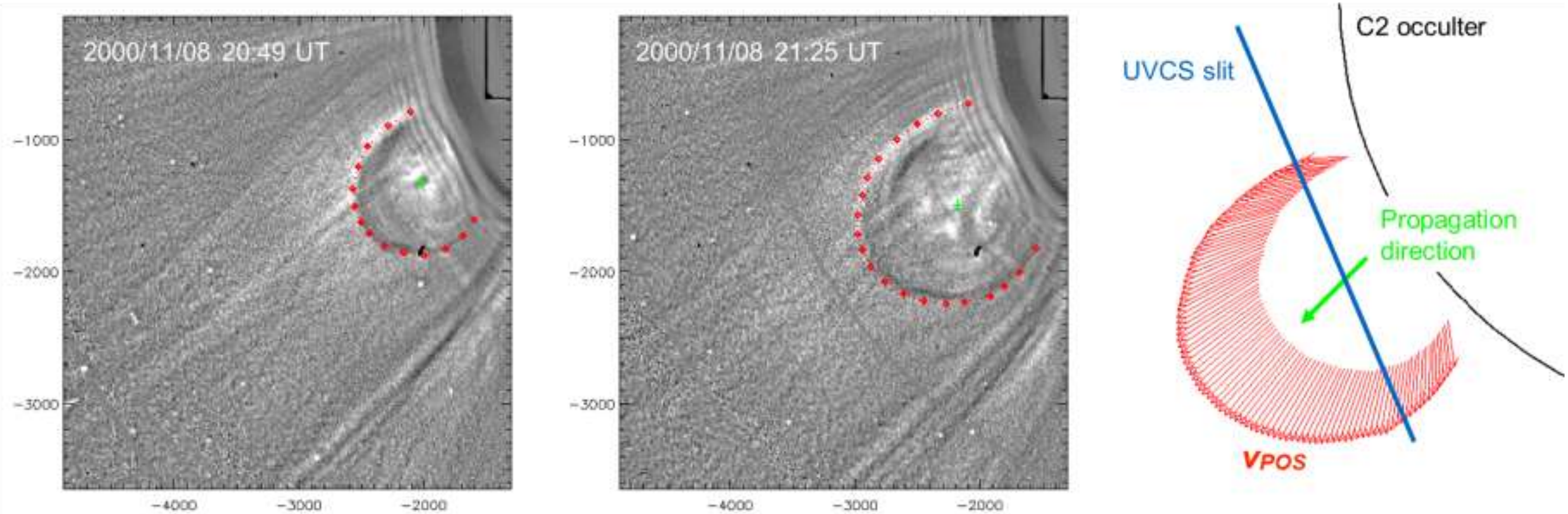

- Approximate estimate of plasma velocity is simply provided by the **POS component of the CME speed**
- v_{POS} is determined by **locating homologous points along the front** at the two different times and computing **height-to-time ratios**
- **Deprojection** is peformed using information derived with the polarization-ratio technique

$$v_{\text{out}} = \frac{v_{\text{POS}}}{\cos\varphi} = v_{\text{POS}} \frac{\sqrt{\varrho^2 + z^2}}{\varrho}$$

T_e in CMEs from WL and UV Lyα intensities

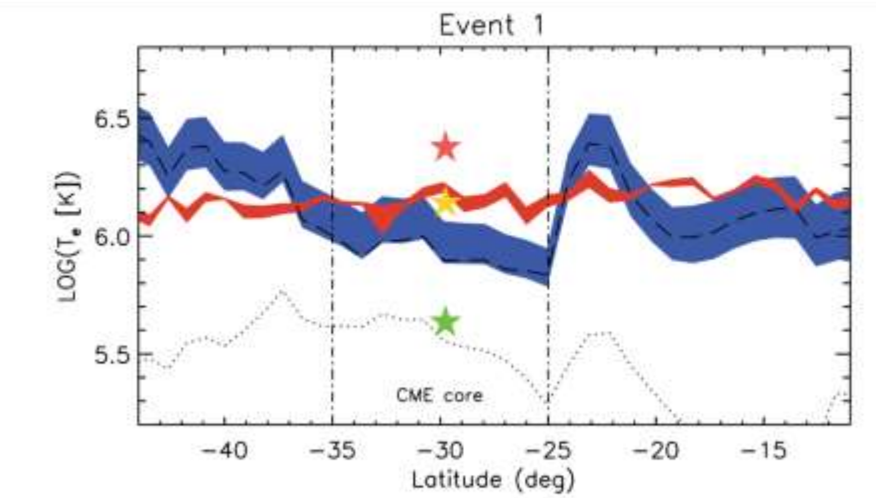

H I T_k (upper limit)
T_e
T_e from collisional component
Akmal et al. (2001)
Ciaravella et al. (2003)
Bemporad et al. (2007)

- Electron temperature in the range $10^{5.8}$–$10^{6.5}$ K
- T_e is **lower in the core**, but quite high value than typical measurements
- Temperature peak (~ $10^{6.5}$ K) consistent with the position of the CME front → **signature of heating by plasma compression?**
- Temperature increase associated with the CME void ($T_e > 10^6$) consistent with previous measurements (> $10^{6.2}$ K by Ciaravella et al. 2003)
- T_e from **collisional component is a lower limit to real temperature**

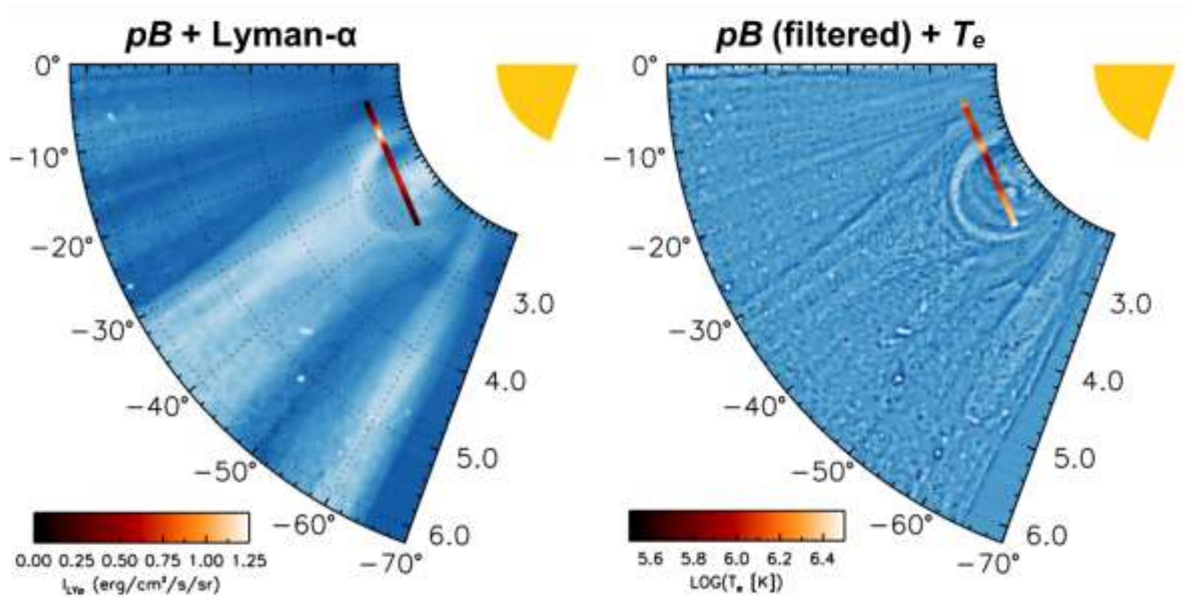

Shows an example of future data analysis that will be performed with Metis observations of CMEs

2D distribution of CME speed on the POS

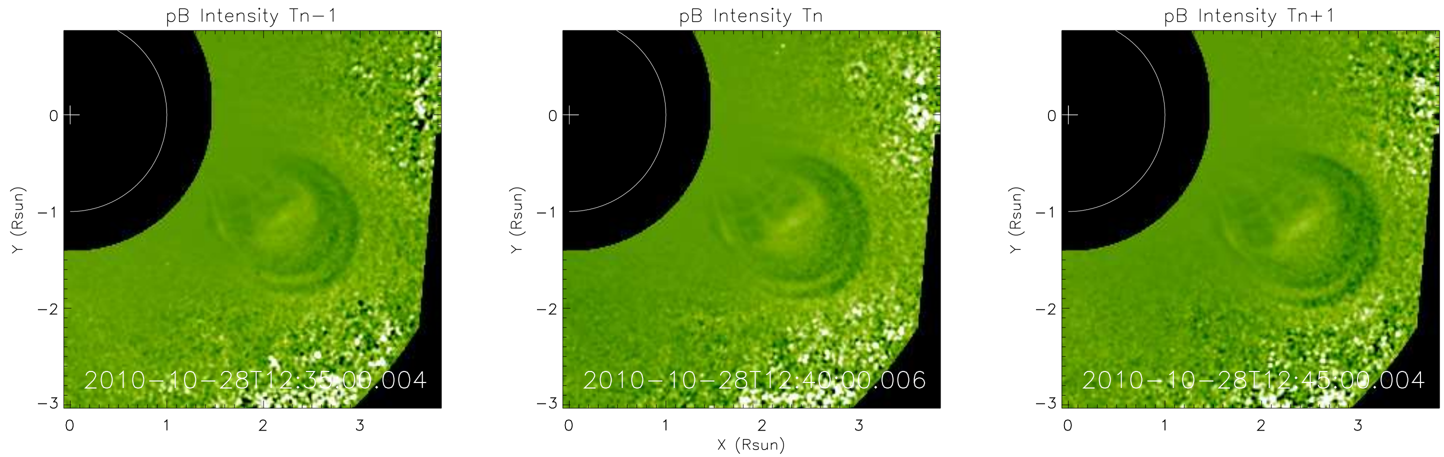

CME plane-of-sky speed

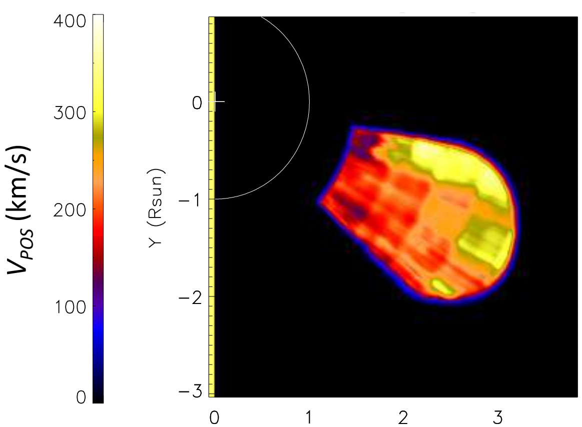

CME Lyα DD factors

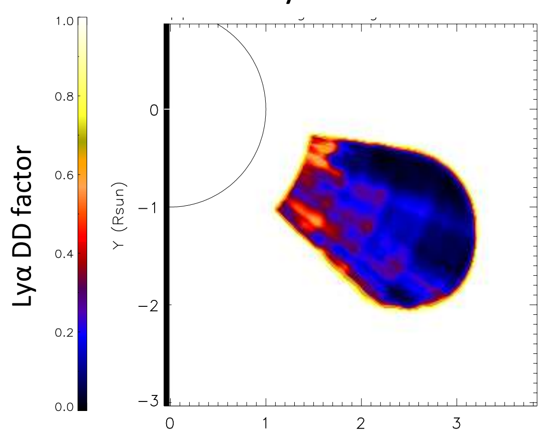

This work demonstrate for the first time how **coronagraphic images** can be analysed to derive **2D maps of the almost instantaneous plasma POS speed** within the body of CMEs.

The derived 2D speed maps have been employed to derive the expected **2D distribution of Lyα Doppler dimming** coefficients for UV Lyman-alpha intensity due to radiative excitation, confirming that (as recently shown by Bemporad et al. 2018) the UV intensity in the CME front will be severely attenuated due to the larger plasma radial speed.

(Ying et al. 2019 in prep. → see poster presentation)

3) Tests with synthetic observations of CMEs

Synthetic WL and UV Lyα CME images

- **3D MHD Spherical simulation** (128x128x256 pts).
- Dense and cold magnetic **flux rope formed** (by differential rotation, meridional flows and surface diffusion) **and ejected** because of initial magnetic configuration out of equilibrium.
- Coupling of Global Model (flux rope formation) + AMRVAC (CME) (Pagano et al., 2013).

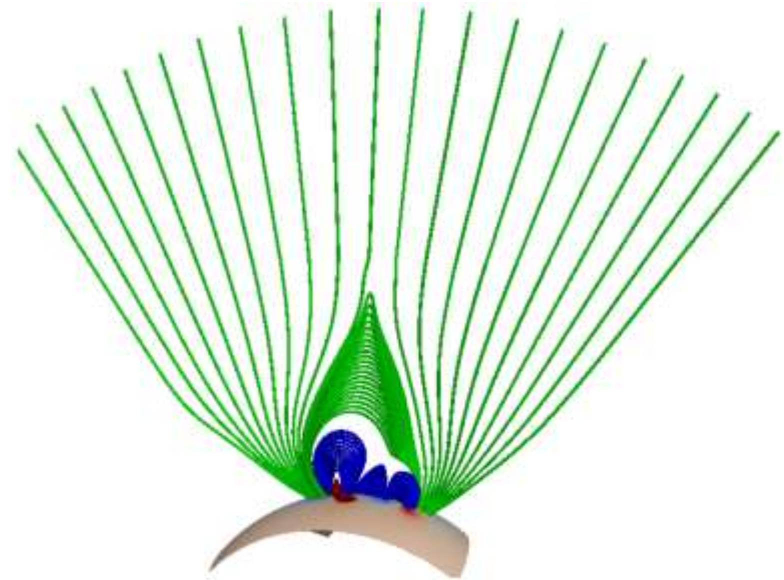

Density Temperature

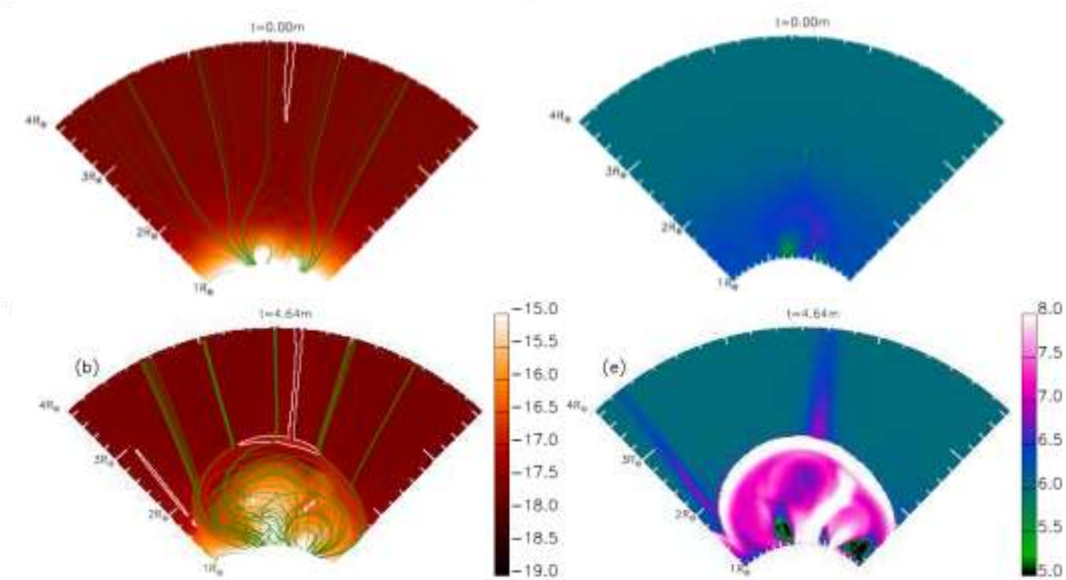

- The flux rope is ejected out of the corona, producing a **fast CME** (2000 km/s) and a propagating hot and dense front.
- The **flux rope** is initially at $10^{5.5}$ K, **is heated** (by numerical mag. diffusivity) to $10^{7.5}$ K and it finally cools down to $10^{6.2}$ K.

Synthetic WL and UV Lyα CME images

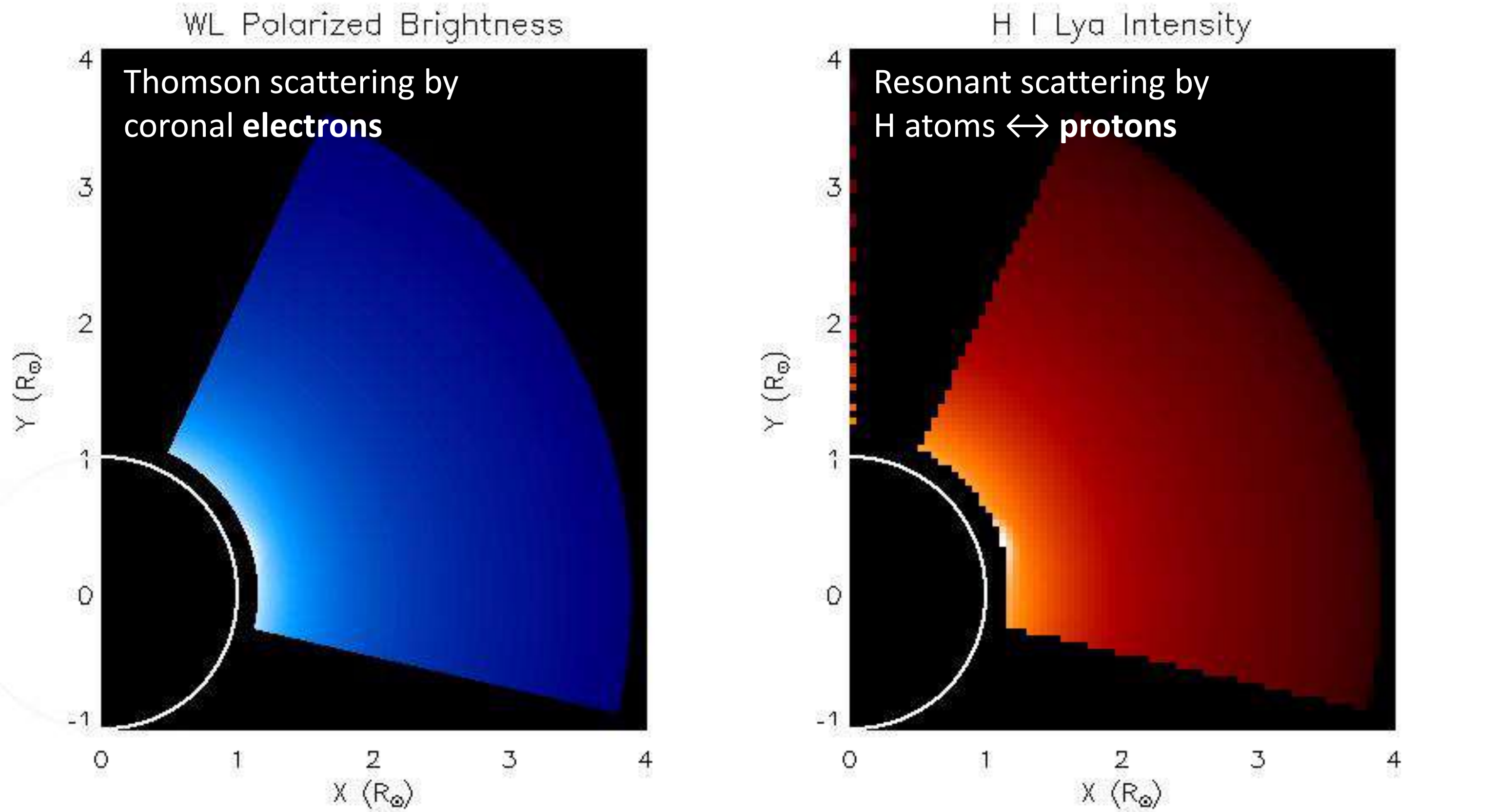

3D MHD simulation performed with a flux rope expanding in a gravitationally stratified corona (**P. Pagano**); **Lyman-alpha emissivities** computed with density, temperature, velocity datacubes, for optically thin plasma, and neglecting T anysotropies, solid angle integration, out-of-equilibrium (**S. Giordano**).

CME front: brigth in WL, dark in UV due to **expansion velocity** (Doppler dimming) effect
CME core: bright in WL, much brighter in UV due to **temperature** effect

Synthetic WL and UV Lyα CME images

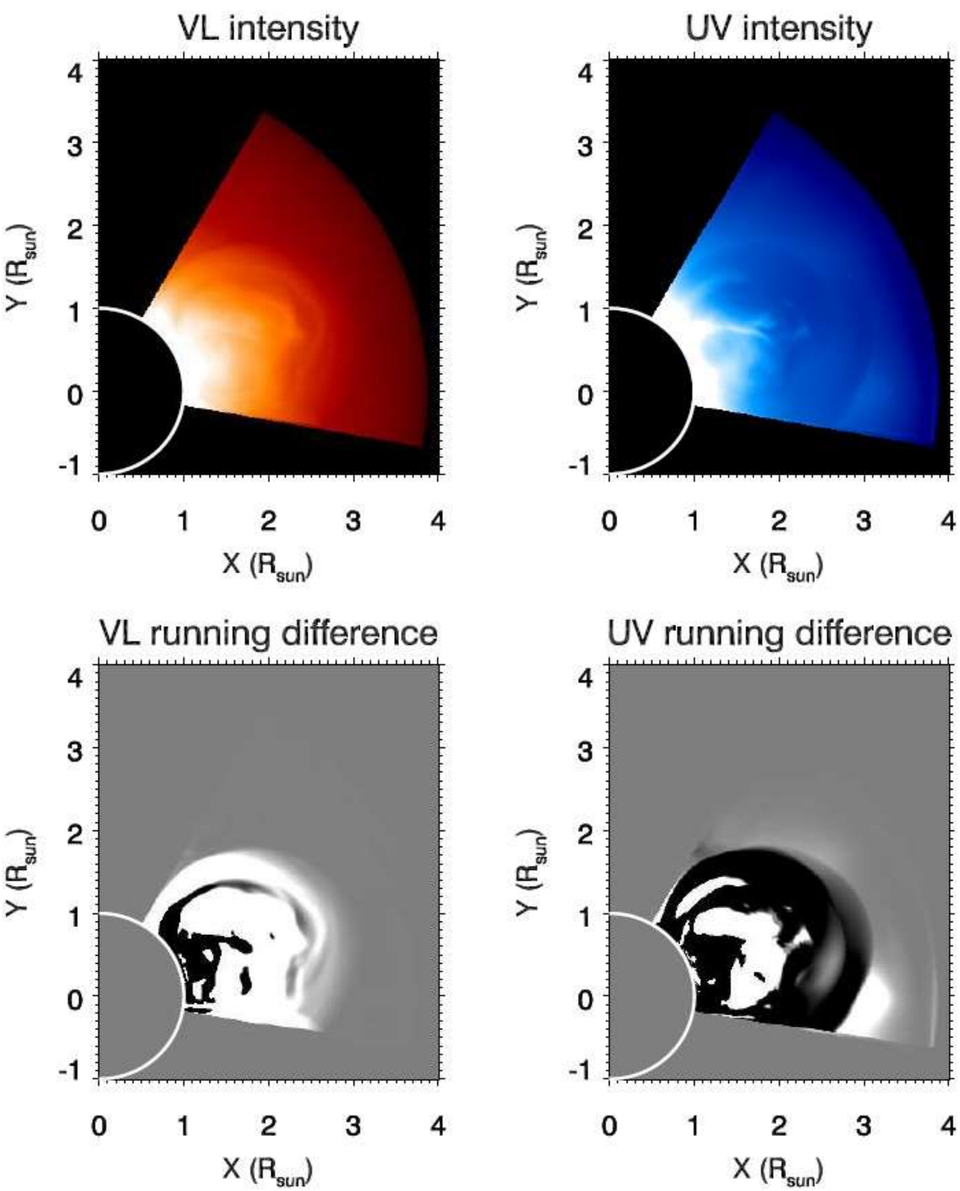

Appearance of the CME front in the two channels is completely different: the VL channel shows the classical arch-shaped, bright expanding front, while the **UV channel shows the expansion of a dark arch-shaped area**, spatially coincident with the VL front.

This difference between VL and UV is mainly due to the **Doppler dimming** effect; moreover, for the CME simulated here, plasma temperatures at the front are significantly larger with respect to the rest of CME body, and this results in a reduced number density of neutral H atoms, and thus reduced Ly-α radiative and collisional emissions.

(Bemporad et al. 2018)

Testing CME temperature estimate from UV

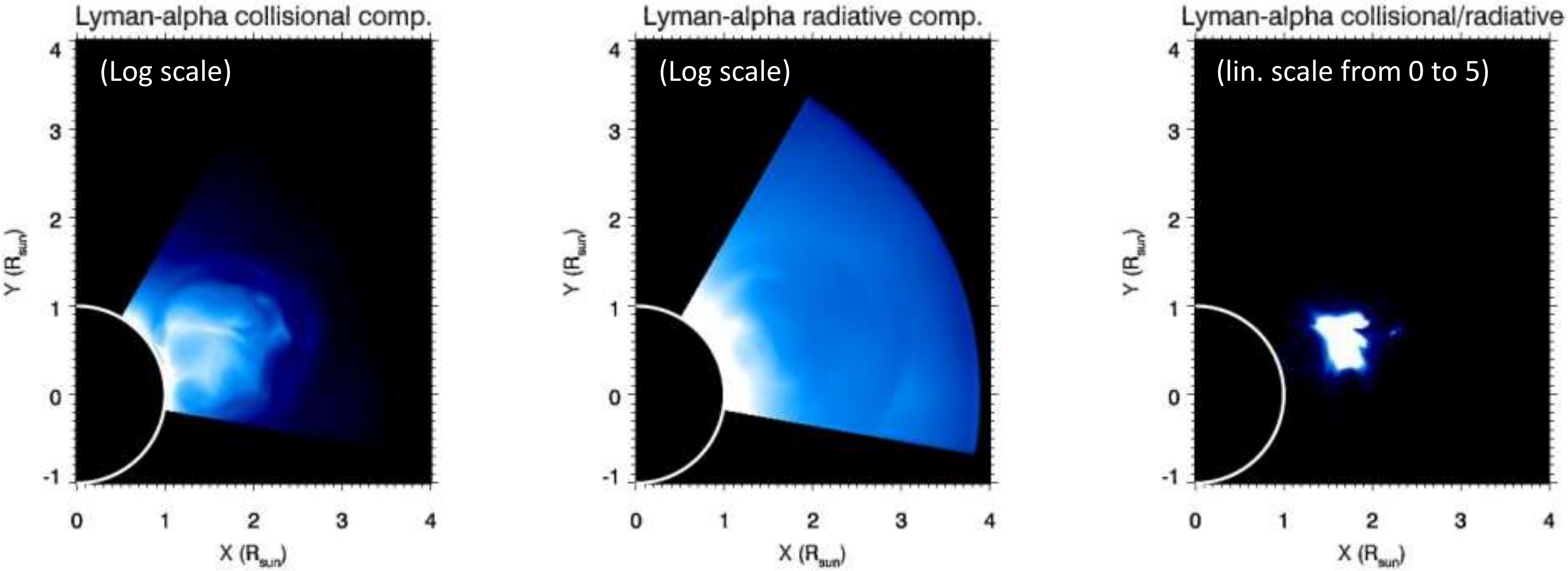

In the inner part of the CME the **Lyα collisional component is dominant**, while in the CME front the Lyα emission will be very low in both the collisional and radiative components → totally different from what happens usually in the stationary solar corona, where the Lyα collisional component is negligible.

Method: output temperatures derived by assuming fully collisional (T_e(**FCE**)), fully radiative (T_e(**FRE**)), or a combination of radiative and collisional excitations (T_e(**RCE**)), and compared with input temperatures averaged along the LOS (T_e(**LOS**)), weighted with the density (T_e(**LOSn**)), and density squared (T_e(**LOSn2**)).

Testing CME temperature estimate from UV

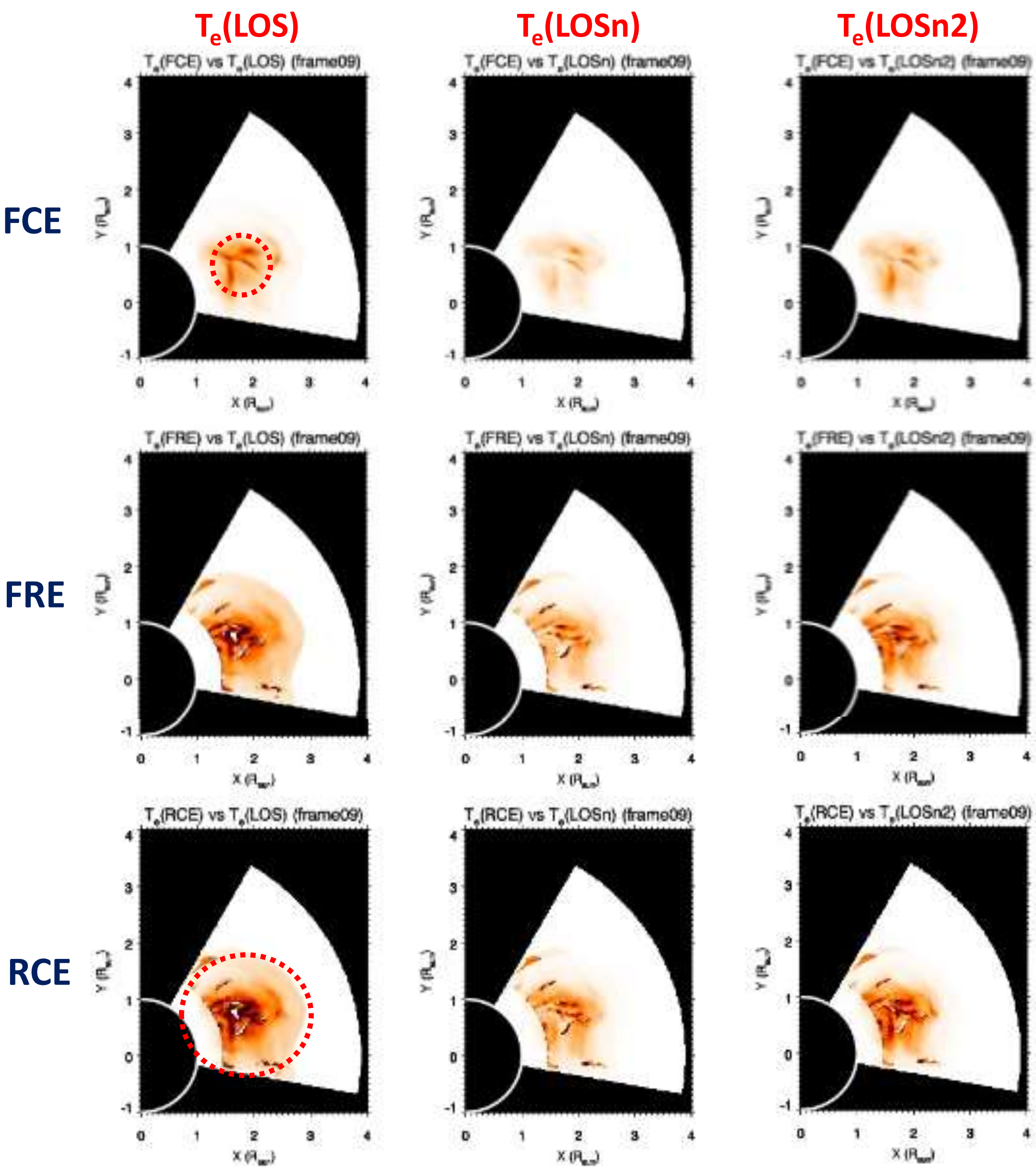

← "black" = "better agreement" scale from 0 to 100%

Results: output temperatures are in general **underestimated** (50%-80%) with respect to the input temperatures, whatever method is considered to account for LOS effects.

The **FCE** approximation is relatively good in the **CME core** and for all the CME parts expanding much faster than ~ 300 km/s. For the rest of the CME the **RCE** approximation works much better.

Shows future difficulties in the interpretation of CME temperatures that will be derived with Metis data.

Future: testing ionization eq. in CMEs

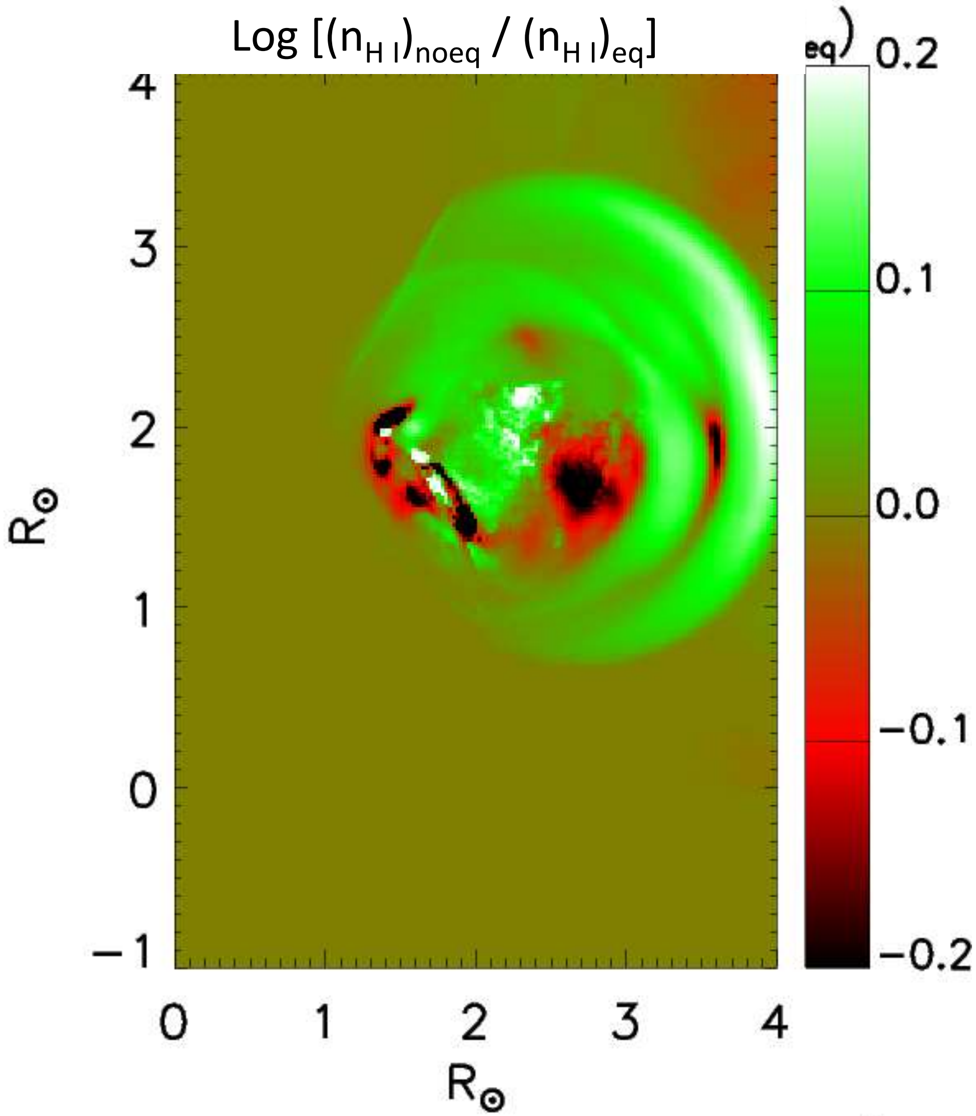

In the analysis of UV and EUV observations of CMEs **ionization equilibrium** is almost always assumed → this assumption is responsible for significant uncertaintines.

To test this a **MHD simulation** of the effects of **loss of ionization equilibrium** in an expanding CME is being performed (based on method by **Pagano 2008**) → out-of-equilibrium we expect a **larger fraction of neutral H at the CME front (factor ~1.6)**, a lower fraction at the flanks (~0.6), and almost the same fraction at the core → important **consequences on temperature determinations** based on the combined analysis of WL and UV coronagraphic images.

Also the role of **photo-ionization** could play an important role for prominences in CME cores (see **next talk**).

Summary

1. Tests with real observations of CMEs: once **CME density** is inferred and **v_{POS} is measured** and deprojected with CME propagation angle derived with polarization ratio, **CME temperatures** can be inferred.

2. Tests with synthetic observations of CMEs: output temperatures are in general **underestimated** (50-80%), fully collisional approximation works quite good in the CME core and in faster (> 300 km/s) CME regions.

3. Similar analyses on real data will open new capability of "**CME temperature imaging**", allowing to study plasma heating/cooling occurring in different parts of CMEs during their expansion.

4. **Further efforts** are going on to understand the **future interpretation** of CME temperatures that will be derived with Metis data, including departures from ionization equilibrium, UV optical thickness, photo-ionization, etc…